Chaotic motion in a flexible rotating beam and synchronization

B. Sandeep Reddy [*], Ashitava Ghosal [†]

Abstract

A rotating flexible beam undergoing large deformation is known to exhibit chaotic motion for certain parameter values. This work deals with an approach for control of chaos known as chaos synchronization. A nonlinear controller based on Lyapunov stability theory is developed and it is shown that such a controller can avoid the sensitive dependence of initial conditions seen in all chaotic systems. The proposed controller ensures that the error between the controlled and the original system, for different initial conditions, asymptotically goes to zero. A numerical example using the parameters of a rotating power generating wind turbine blade is used to illustrate the theoretical approach
Keywords: Multiple scales analysis, Chaos synchronization, Lyapunov Stability

1 Introduction

A nonlinear dynamical system characterized by sensitivity to initial conditions for certain parameter values is termed as a chaotic system. This phenomenon is seen in several physical, chemical, biological and engineered systems. Some of the most well-known examples are the Duffing's equation [1, 2] with a nonlinear (cubic) spring stiffness term, a double pendulum and two-degree-of-freedom robot manipulators [3, 4]. Chaotic motions are also seen in a rotating flexible beam [5] undergoing large deformation. Chaos in a system leads to unpredictability and, in engineered systems, can lead to failure. Controlling chaos systems has thus received a significant amount of attention and many approaches [6, 7, 8, 9, 10, 11, 12, 13] have been proposed. In the recent past, a form of chaos control termed chaos synchronization has also received attention [14, 15]. In chaos synchronization approaches, a system with one given set of initial conditions is termed as the drive system and another identical system with a different set of initial conditions is termed as the response system. In the absence of a controller, the drive and response systems will diverge due to the property of sensitivity to initial conditions. The central idea of synchronization is to design a controller such that the response system asymptotically tracks the drive system. A number of approaches have been proposed for synchronizing chaotic systems such as back-stepping design [16], adaptive control [17], sliding mode control [18] and robust feedback control [19]. Global chaos synchronization was studied using sliding mode control [20, 21] on the Li-Wu and the Zhu systems respectively. Chaos synchronization of chaotic Chua system with cubic nonlinearity in complex coupled networks [22] and modified projective synchronization of different order chaotic systems with adaptive scaling factor [23] were also studied. In this paper we use active nonlinear control and Lyapunov stability theory to design a controller for the chaotic system arising from a model of a power generating wind turbine blade. In this paper, following the development in reference [5], the rotating wind turbine blade is modeled as four first-order ordinary differential equations (ODEs) in a non-dimensional form using two characteristic velocities. The non-dimensional equations of motion of a rotating beam undergoing large deformation follows from the work in reference [24]. The method of multiple scales [25] is used to analyze these four first-order ODEs at various time scales to obtain four first-order autonomous slow flow equations. These equations are shown to be chaotic for certain ranges of values of these characteristic velocities [5]. The main and new contribution of this paper is the development of control laws which synchronize the chaotic system. The control laws are obtained by designing a nonlinear controller using nonlinear control and Lyapunov stability theory. Numerical simulation results are used to validate the approach described in this paper.

[*]Graduate Student, Department of Mechanical Engineering, Indian Institute of Science, Bangalore, India. Email: bsandeep@mecheng.iisc.ernet.in

[†]Corresponding Author, Professor, Department of Mechanical Engineering, Indian Institute of Science, Bangalore, India. Email: asitava@mecheng.iisc.ernet.in

The paper is organized as follows. In section 2, for the sake of completeness, we present the model of a rotating wind turbine blade as a flexible rotating beam undergoing large deformation and the four first-order ODEs which model this nonlinear system. In section 3, we perform an analysis of the slow flow equations obtained for the equations of the beam using the method of multiple scales, and explain certain insights which are relevant to chaos synchronization. In section 4, we design the nonlinear controller using Lyapunov stability theory for chaos synchronization. In section 5, we present numerical simulation results of the controller. In section 6, we present the conclusions to this paper.

2 Modeling of a wind turbine blade as a rotating flexible beam

The modeling of a rotating flexible link, undergoing large deformation and the detailed derivation of its equations of motion in a non-dimensional form are available in reference ([24, 5]). These are presented in brief in this section for the sake of completeness.

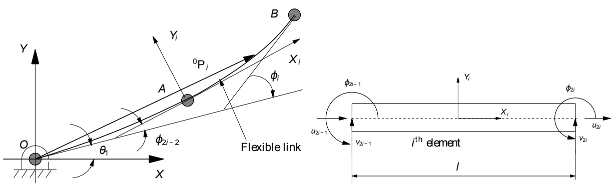

(a) Flexible rotating beam (b) Planar beam element

Figure 1: Schematic of a rotating flexible beam(from [5])

The rotating flexible link is schematically shown in figure 1(a), discretized into N number of elements, OA, AB and so on. The equation of motion of the rotating link, modeled as a slender rotating beam undergoing transverse bending vibration, can be derived as a partial differential equation using Euler-Bernoulli beam theory. In this work, we model the beam as a single element (OB) and hence $i = 1$ in both figure 1 (a), (b). Figure 1(b) shows the various nodal degrees of freedom on the beam element OB. The nodal variables $(u_1, v_1, \phi_1, u_2, v_2, \phi_2)$, as described in figure 1(b) are defined in the body fixed co-ordinate system X_1Y_1. The variables (u_1, v_1, u_2, v_2) represent the nodal displacements (along the X and Y directions respectively, as shown in figure 1(b)), while (ϕ_1, ϕ_2) represent nodal rotations. The co-ordinate system OXY shown in figure 1(a) is the global reference co-ordinate system and $^0\mathbf{P}_i$ is the position vector of a point in the beam element.

The rotating flexible link is assumed to have constant cross-sectional area and uniform material properties. It is assumed to undergo axial elongation in addition to transverse bending. In figure 1(a), θ_1 is the rigid body (rotation) variable and for clamped boundary conditions ($u_1 = v_1 = \phi_1 = 0$). The total number of variables describing the rotating beam will be four – one rigid body variable (θ_1) and three flexible variables denoted by $Q_f = (u_2, v_2, \phi_2)$. We denote the set of four variables $(\theta_1, u_2, v_2, \phi_2)$ by Q.

The equations of motion in the non-dimensional form can be written as (see reference [24])

$$[\mathcal{M}(Q_f)]\ \{Q^{''}\} + \left(\mathcal{K} + \Delta\mathcal{K}(Q_f, \frac{U_a}{U_g})\right) \{Q\} + \mathcal{C}\{Q'\} + \{\mathcal{H}(Q, Q^{'})\} = \frac{\{\tau\}}{\rho A L U_g^2} \quad (1)$$

where $(\cdot)^{'}, (\cdot)^{''}$ represent the first and the second derivative with respect to non-dimensional time T, $\mathcal{M}$ is the 4×4 non-dimensional mass matrix, $\mathcal{K}$ and $\Delta\mathcal{K}$ are the 4×4 non-dimensional conventional and geometric stiffness matrices respectively, $\mathcal{H}$ is the 4×1 vector of non-dimensional centripetal and Coriolis terms, $\{\tau\} = [F \sin(\frac{\Omega L}{U_g} T), 0, 0, 0]^T$ with F and Ω denoting the amplitude and the frequency of forcing term (see [24, 5] for details of the terms in equation (1)) and $\mathcal{C}\{Q'\}$ represents an added Rayleigh damping term of the form $\alpha[\mathcal{M}] + \beta[\mathcal{K}]$.

The non-dimensional equations of motion (1) contain two characteristic velocities

$$U_g = \frac{1}{L}\sqrt{\frac{EI}{\rho A}}, \quad U_a = \sqrt{\frac{E}{\rho}}, \quad T = t/(L/U_g) \quad (2)$$

where U_a is the phase speed of the longitudinal wave or the speed of sound in the material and U_g is a characteristic velocity associated with bending vibration and the non-dimensional time T is given by $t/(L/U_g)$.

For numerical simulations in section 5, we will use the values given in Table 1 and we assume the value of amplitude of forcing $F = \pi/2$ and the values of the Rayleigh damping coefficients as $\alpha = 0.02$ and $\beta = 0.02$. It may be noted that the ρ and E values given in Table 1 are of E-glass which is used to make the power generating wind turbine blades and the value of L is given for a 50 kW wind turbine made by Endurance Wind Power Ltd. [26]. The value of Ω is the operating angular speed of the wind turbine blade. It may be noted that in an actual wind turbine blade the cross-section is not uniform, the blade undergoes twisting in addition to bending and there are other nonlinearities in the drive and control system which are not considered in the model. In this work, we show that the system of four nonlinear ODEs in equation (1) can exhibit chaos for certain parameter values and we present controllers to illustrate synchronization of chaos.

3 Analysis of the equations of the rotating beam

To analyze the behavior of the beam, we use the method of multiple scales (MMS) [25] and derive the slow flow equations (see [5] for details). These are given by

$$\begin{aligned}
\dot{x} &= -\frac{\alpha x}{2} - \sigma_1 y + 2J_{32}xy + 2J_{31}\frac{yw}{z^2+w^2} \\
\dot{y} &= -\frac{\alpha y}{2} + \sigma_1 x - J_2(z^2+w^2) - 2J_{32}x^2 - \frac{2J_{31}xw}{z^2+w^2} \\
\dot{z} &= -J_{3d}z - \sigma_2 w + J_{31} + J_{32}(xw - yz) \qquad (3)\\
\dot{w} &= -J_{3d}w + \sigma_2 z - J_{32}(yw + xz)
\end{aligned}$$

where (x, y, z, w) are the slow flow variables which are dependent on original variables $(\theta_1, u_2, u_2, \phi_2)$ (as shown in figure 1), J_{3d} is a function of Rayleigh damping co-efficients (α, β), while (σ_1, σ_2) are the detuning parameters. The complete expressions for the terms are available in reference [5] and in this paper we analyze equations (3) and present a scheme to synchronize chaos in these equations.

We can make the following observations about the above nonlinear differential equations (3).

1. The variables (θ_1, V_2, ϕ_2) are functions of amplitude a_3 and phase b_3, whereas global variable U_2 is a function of amplitude a_2 and phase b_2. The slow flow variables (x, y) are functions of (a_2, b_2, b_3), whereas the variables (z, w) are functions of (a_3, b_3). Thus, if variables (z, w) go to zero, then the original variables (V_2, ϕ_2) (see figure 1) will also go to zero. It will be seen in section 5 that the variables do go to zero irrespective of the value of parameter U_g.

2. The first two equations contain a factor $\frac{w}{z^2+w^2}$. As a result, as shown in simulation results (see section 5), the behavior of $x(t)$ and $y(t)$ is very different than the behavior of $z(t)$ and $w(t)$.

3. The undamped slow flow equations were found to be chaotic for $U_g < 150$ and the damped slow flow equations were found to be chaotic for $U_g < 200$ (see reference [5] for details).

4. The initial conditions for both the damped and the undamped slow flow equations were taken as $(-0.3538, -1.5771, 0.2820, -1.3337)$.

In the next section, we present a scheme to control chaos, namely chaos synchronization.

4 Chaos synchronization

The hallmark of chaotic systems is sensitivity to initial conditions and a small change in the initial conditions can render the output unpredictable in the long run. In practice, errors in initial conditions are near inevitable and this makes it impossible to predict the state output as time increases. One approach towards more predictability in the state output is by *chaos synchronization*. This can be done by considering two systems – a drive system (theoretical model of the system with given initial conditions) and the response system (practical model of the system with error in the initial conditions with respect to the initial conditions of the drive system), and designing a controller to force the error between the state outputs of the drive and response system to go asymptotically to zero. In this way, the practical and the theoretical systems will be synchronized and the effect of the change in initial conditions is negated.

For equation (3), the drive and response systems can be written as

$$\begin{aligned}
\dot{x_d} &= -\frac{\alpha x_d}{2} - \sigma_1 y_d + 2J_{32}x_d y_d + 2J_{31}\frac{y_d w_d}{{z_d}^2+{w_d}^2} \\
\dot{y_d} &= -\frac{\alpha y_d}{2} + \sigma_1 x_d - J_2({z_d}^2+{w_d}^2) - 2J_{32}{x_d}^2 \\
&\quad - 2J_{31}\frac{x_d w_d}{{z_d}^2+{w_d}^2} \qquad (4)\\
\dot{z_d} &= -J_{3d}z_d - \sigma_2 w_d + J_{31} + J_{32}(x_d w_d - y_d z_d) \\
\dot{w_d} &= -J_{3d}w_d + \sigma_2 z_d - J_{32}(y_d w_d + x_d z_d)
\end{aligned}$$

and

$$
\begin{aligned}
\dot{x_r} &= -\frac{\alpha x_r}{2} - \sigma_1 y_r + 2J_{32}x_r y_r + \frac{2J_{31}y_r w_r}{{z_r}^2 + {w_r}^2} + u_1 \\
\dot{y_r} &= -\frac{\alpha y_r}{2} + \sigma_1 x_r - J_2({z_r}^2 + {w_r}^2) - 2J_{32}{x_r}^2 \\
&- 2J_{31}\frac{x_r w_r}{{z_r}^2 + {w_r}^2} + u_2 \qquad (5) \\
\dot{z_r} &= -J_{3d}z_r - \sigma_2 w_r + J_{31} + J_{32}(x_r w_r - y_r z_r) + u_3 \\
\dot{w_r} &= -J_{3d}w_r + \sigma_2 z_r - J_{32}(y_r w_r + x_r z_r) + u_4
\end{aligned}
$$

where the lower subscript d and r stand for drive and response system respectively, and $u_i,\ i = 1, 2, 3, 4$ are the control which synchronizes the two chaotic systems.

From equations (4) and (5), the error dynamics can be given as

$$
\begin{aligned}
&\dot{e_1} = -\frac{\alpha e_1}{2} - \sigma_1 e_2 + 2J_{32}(x_r e_2 + y_r e_1 - e_1 e_2)+ \\
&2J_{31}\frac{y_r w_r}{{z_r}^2 + {w_r}^2} - 2J_{31}\frac{(y_r - e_2)(w_r - e_4)}{(z_r - e_3)^2 + (w_r - e_4)^2} + u_1 \\
&\dot{e_2} = -\frac{\alpha e_2}{2} + \sigma_1 e_1 - J_2(e_3(2z_r - e_3)+ \\
&e_4(2w_r - e_4)) - 2J_{32}(e_1(2x_r - e_1)) - 2J_{31}\frac{x_r w_r}{{z_r}^2 + {w_r}^2} \\
&\quad + 2J_{31}\frac{(x_r - e_1)(w_r - e_4)}{(z_r - e_3)^2 + (w_r - e_4)^2} + u_2 \qquad (6)
\end{aligned}
$$

$$
\begin{aligned}
\dot{e_3} &= -J_{3d}e_3 - \sigma_2 e_4 + J_{32}(x_r e_4 + w_r e_1 - e_1 e_4 \\
&- y_r e_3 - z_r e_2 + e_2 e_3) + u_3 \\
\dot{e_4} &= -J_{3d}e_4 + \sigma_2 e_3 - J_{32}(x_r e_3 + z_r e_1 - e_1 e_3 \\
&+ y_r e_4 + w_r e_2 - e_2 e_4) + u_4
\end{aligned}
$$

where $e_1 = x_r - x_d$, $e_2 = y_r - y_d$, $e_3 = z_r - z_d$ and $e_4 = w_r - w_d$.

For the two identical chaotic systems without control or $u_i = 0$, if the initial conditions are not equal, i.e., $(x_d(0), y_d(0), z_d(0), w_d(0)) \neq (x_r(0), y_r(0), z_r(0), w_r(0))$, then the trajectories of the two identical systems will diverge with respect to each other. However under control, the two systems will synchronize with each other for any initial conditions, implying that error states asymptotically go to zero. For this end, we must propose the use of a control input $u = [u_1, u_2, u_3, u_4]^T$ which makes the error states asymptotically go to zero.

Using the Lyapunov second method for stability, consider the candidate Lyapunov function

$$V = (1/2)({e_1}^2 + {e_2}^2 + {e_3}^2 + {e_4}^2) \qquad (7)$$

The differential of the Lyapunov function along the trajectory of the system is

$$\dot{V} = e_1\dot{e_1} + e_2\dot{e_2} + e_3\dot{e_3} + e_4\dot{e_4} \qquad (8)$$

Using (6), we get

$$
\begin{aligned}
&\dot{V} = -\frac{\alpha}{2}{e_1}^2 - \frac{\alpha}{2}{e_2}^2 - J_{3d}{e_3}^2 - J_{3d}{e_4}^2 \\
&+ J_{32}(y_r(2{e_1}^2 - {e_3}^2 - {e_4}^2) - 2x_r e_1 e_2) \\
&+ (J_{32} + J_2)e_2({e_3}^2 + {e_4}^2) - z_r(e_2 e_3(J_{32} + J_2) \\
&+ J_{32}e_1 e_4) + w_r(e_1 e_3 J_{32} - (J_{32} + J_2)e_2 e_4)+ \qquad (9) \\
&2J_{31}(x_r e_2 - y_r e_1)Q_1 + u_1 e_1 + u_2 e_2 + u_3 e_3 + u_4 e_4
\end{aligned}
$$

where

$$Q_1 = \left(\frac{w_r - e_4}{(z_r - e_3)^2 + (w_r - e_4)^2} - \frac{w_r}{(z_r)^2 + (w_r)^2}\right) \qquad (10)$$

For asymptotic stability according to Lyapunov second method, we must have $V > 0$ and $\dot{V} < 0$. It can be seen from equation (7) that $V > 0$. To ensure $\dot{V} < 0$, the control input $u = [u_1, u_2, u_3, u_4]^T$ in equation (9) must be designed accordingly. Hence, we propose the following control law,

$$
\begin{aligned}
&u_1 = \left(\frac{\alpha}{2} - 1\right)e_1 + J_{32}(2e_2 x_r - 2e_1 y_r + e_4 z_r - \\
&e_3 w_r) + 2J_{31}y_r Q_1,\ u_2 = \left(\frac{\alpha}{2} - 1\right)e_2 - (J_{32} + J_2) \\
&({e_3}^2 + {e_4}^2) + (J_{32} + 2J_2)(e_3 z_r + e_4 w_r) - 2J_{31}x_r Q_1 \\
&u_3 = (J_{3d} - 1)e_3 + J_{32}y_r e_3 \qquad (11) \\
&u_4 = (J_{3d} - 1)e_4 + J_{32}y_r e_4
\end{aligned}
$$

Substituting (11) into (9), we have

$$\dot{V} = -{e_1}^2 - {e_2}^2 - {e_3}^2 - {e_4}^2 < 0 \qquad (12)$$

and we can obtain asymptotic stability in the sense of Lyapunov, i.e., the chaotic systems (4) and (5) are synchronized for any initial conditions with the use of the control law (11).

Motivation for the choice of the control law

Equation (12) shows that the control law (11) can synchronize the chaotic systems (4) and (5) for any initial conditions. The motivation for the choice of the control law is based on the following observations.

1. Equation (9) contains constant terms such as (J_2, J_{31}, J_{32}) and varying terms (x_r, y_r, z_r, w_r) which could be negative or positive. Since, for asymptotic stability we must have $\dot{V} < 0$, these varying terms must be eliminated using the control input u_i.

2. It can be seen from equation (9) that there are coupled error and control input terms of the form $u_i e_i$. To eliminate the constant and varying terms, the control law should not contain fractions with an error or varying term in the denominator. For example, a choice of $u_3 = \dfrac{2J_{32}x_r e_1 e_2}{e_3}$ can cancel $(-2J_{32}x_r e_1 e_2)$ in equation (9). However, if $e_3 \to 0$, then u_3 would go to infinity. A better choice would be $u_1 = 2J_{32}x_r e_2$. In general, an u_i should be chosen to cancel out terms containing corresponding e_i to which it is coupled to. If the terms contain combination of errors, such as the term $(-2J_{32}x_r e_1 e_2)$, then the controller u_1 or u_2 can be designed to cancel out such a term.

3. The simpler the controller, the better.

In equation (9), the presence of terms such as (e_1^2, e_3^2, e_4^2) can be seen. This implies that in order to cancel those terms out, we must make use of control inputs (u_1, u_3, u_4). There is only one term containing e_2^2 and the control input u_2 is necessary only to cancel out that term. The control law (11) satisfies all the above three conditions.

It is possible however to design other control laws. Consider another control law of the form

$$
\begin{aligned}
&u_1 = (\alpha/2 - 1)\, e_1 + J_{32}(2e_2x_r - 2e_1y_r + e_4z_r - e_3w_r)\\
&+ 2J_{31}y_rW_{x1}, u_2 = (\alpha/2 - 1)\, e_2, u_3 = (J_{3d} - 1)e_3\\
&+ J_{32}y_re_3 + (J_{32} + 2J_2)z_re_2 - (J_{32} + J_2)e_2e_3 -\\
&2J_{31}x_rW_{x2},\ u_4 = (J_{3d} - 1)e_4 + J_{32}y_re_4 + \\
&(J_{32} + 2J_2)w_re_2 - (J_{32} + J_2)e_2e_4 - 2J_{31}x_rW_{x3}
\end{aligned}
\tag{13}
$$

where

$$
\begin{aligned}
W_{x1} &= \frac{e_3w_r(2z_r - e_3) + e_4(w_r(w_r - e_4) - z_r^2)}{((z_r - e_3)^2 + (w_r - e_4)^2)(z_r^2 + w_r^2)}\\
W_{x2} &= \frac{e_2w_r(2z_r - e_3)}{((z_r - e_3)^2 + (w_r - e_4)^2)(z_r^2 + w_r^2)}\\
W_{x3} &= \frac{e_2(w_r(w_r - e_4) - z_r^2)}{((z_r - e_3)^2 + (w_r - e_4)^2)(z_r^2 + w_r^2)}
\end{aligned}
\tag{14}
$$

On substitution of equation (13) into equation (9), we get $\dot{V} < 0$ and asymptotic stability can be obtained. However, it can be seen that the control law (13) is more complicated than (11). Since it is preferable to have simpler controllers over complicated ones, we prefer control law (11).

In the next section, we present numerical simulation results illustrating synchronization.

5 Numerical Simulation

In this section we, verify the effectiveness of the control law proposed in section 4. We numerically simulate equations (4), (5), and (6) from section 4. To perform the numerical simulation, we use the parameters given in reference [5]. All simulations are done in MATLAB 2012Rb (Matlab Version 8.0) [27]and *ode*15*s* solver was used to solve the differential equations. The relative and absolute tolerances were kept at 10^{-6} and 10^{-9} respectively.

For all numerical simulations in this section, we use the MATLAB command *randi* to generate random initial conditions. For one such set of initial conditions for $(x_d(0), y_d(0), z_d(0), w_d(0))$ and $(x_r(0), y_r(0), z_r(0), w_r(0))$ given by $(-0.3538, -1.5771, 0.2820, -1.3337)$ and $(-0.34, -1.5771, 0.2820, -1.3337)$, respectively, figures 2 and 4 display the error variables without control and figures 3 and 5 display the error variables with control. As it can be seen, with the controller the error converges to zero, implying the response system is asymptotically tracking the drive system. For both the undamped and damped slow flow equations, we have used $U_g = 100$ in the numerical simulations.

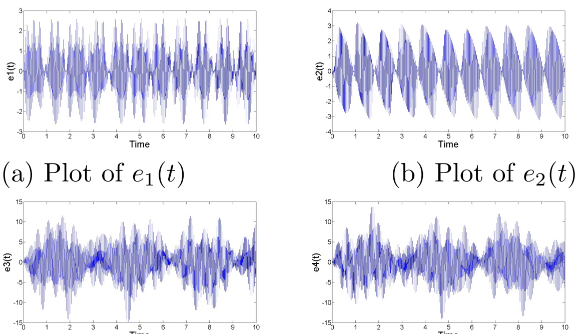

(a) Plot of $e_1(t)$ (b) Plot of $e_2(t)$

(c) Plot of $e_3(t)$ (d) Plot of $e_4(t)$

Figure 2: Synchronization errors *without control* for the undamped equations

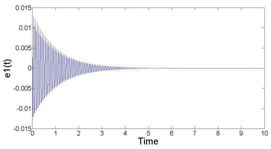

(a) Plot of $e_1(t)$

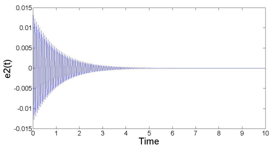

(b) Plot of $e_2(t)$

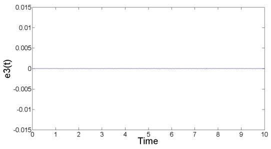

(c) Plot of $e_3(t)$

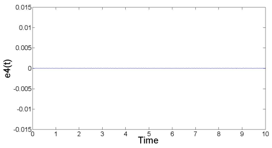

(d) Plot of $e_4(t)$

Figure 3: Synchronization errors *with control* for the undamped equations

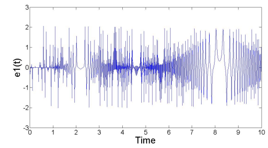

(a) Plot of $e_1(t)$

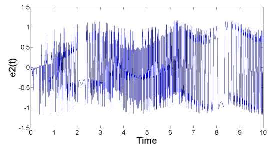

(b) Plot of $e_2(t)$

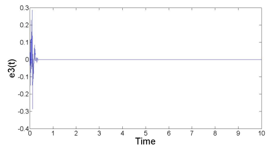

(c) Plot of $e_3(t)$

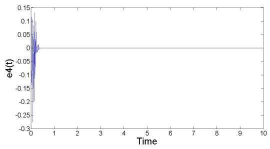

(d) Plot of $e_4(t)$

Figure 4: Synchronization errors *without control* for the damped equations

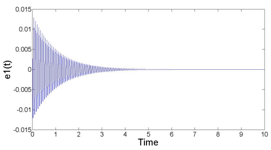

(a) Plot of $e_1(t)$

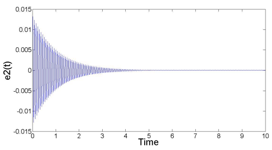

(b) Plot of $e_2(t)$

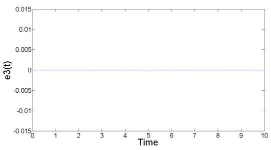

(c) Plot of $e_3(t)$

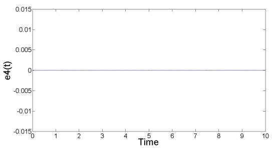

(d) Plot of $e_4(t)$

Figure 5: Synchronization errors *with control* for the damped equations

It is evident from figure 2, that the undamped slow flow equations have large differences in the state variables without the use of the proposed controller. With the use of the control law given in equation (11), the errors converge asymptotically to zero as shown in figure 3.

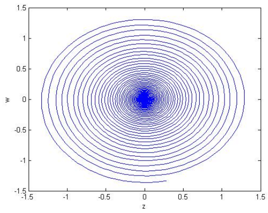

(a) $U_g = 400$

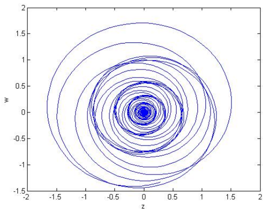

(b) $U_g = 100$

Figure 6: Phase plots for the damped equations showing both the z, w state variables going to zero

It is interesting to observe that for the damped slow flow equations, the errors $e_3(t)$ and $e_4(t)$ (related to $z(t)$ and $w(t)$) go to zero even without the controller (see figure 4 (c) and (d)). This can be seen more clearly from figure 6, that irrespective of the chaoticity, the two state variables z, w tend to zero – the spiral trajectory in the $z - w$ plane.

The numerical simulation results validate control law (11) by successfully demonstrating asymptotic convergence of errors between the drive and response systems to zero.

6 Conclusions

In this paper, we demonstrate chaos synchronization of a system of four nonlinear ordinary differential equations. The equations are derived from a nonlinear model of a rotating flexible beam and are related to the rotating blade of power generating wind turbine. The method of multiple scales is used to derive the slow flow equations for a damped and undamped rotating flexible link. The flexible rotating beam can exhibit chaos for certain values of the parameter U_g. A nonlinear control law for asymptotic chaos synchronization is proposed. The nonlinear control law is derived using Lyapunov stability theory and numerical simulations show the effectiveness of the law in negating the sensitivity to initial conditions for the slow flow equations derived using method of multiple scales. In the future, we aim to develop a unified method for chaos synchronization, depending upon the type of nonlinearity involved in the slow flow equations.

References

[1] Guckenheimer J. and Holmes P., *Nonlinear Oscillations, Dynamical Systems, and Bifurcations of Vector Fields*, Applied Mathematical Sciences, Springer-Verlag, New York, Vol. 42., 1983.

[2] Kovacic I. and Brennan M. J., *The Duffing Equation: Nonlinear Oscillators and Their Behaviour*, 1st ed., John Wiley & Sons, Ltd., 2011.

[3] Burov, A. A., On the non-existence of a supplementary integral in the problem of a heavy two-link plane pendulum, *Prikl. Matem. Mekhan, USSR*, 50(1), pp. 123-125, 1986.

[4] Lankalapalli S. and Ghosal A., Possible chaotic motion in a feedback controlled 2R robot, In *Proceedings of the 1996 IEEE International Conference on Robotics and Automation*, Minneapolis, MN, pp. 1241-1246, 1996.

[5] Reddy B. S. and Ghosal A., Nonlinear dynamics of a rotating flexible link, *Journal of Computational and Nonlinear Dynamics, ASME*, 10(6), pp. 061014, 2015.

[6] Ott E., Grebogi C. and Yorke J. A. , Controlling chaos, *Physical Review Letters*, 64(11), 1196-1199, 1990.

[7] Francisco Heitor Pereira-Pinto I., Armando Ferreira M. and Marcelo Savi A., Chaos control in a nonlinear pendulum using a semi-continuous method, *Chaos Solitions and Fractals*, 22, pp. 653-668, 2004.

[8] De Paula A. S. and Savi M. A., Controlling chaos in a nonlinear pendulum using an extended time-delayed feedback control method, *Chaos, Solitons and Fractals*, 42, pp. 2981-2988, 2009.

[9] Zareiyan Jahromi S. A., Haji A. H. and Mahzoon M., Non-Linear Dynamics and chaos control of a physical pendulum with rotating mass, *13th Annual (International) Mechanical Engineering Conference, Isfahan University of Technology, Isfahan, Iran*, 2005.

[10] Starett J. and Tagg R., Control of a chaotic parametrically driven pendulum, *Physical Review Letters*, 74(11), pp. 1974-1977, 1995.

[11] Pyragas K., Control of Chaos via an Unstable Delayed Feedback Controller, *Physical Review Letters*, 86(11), pp. 2265-2268, 2001.

[12] Alexander Fradkov L. and Robin Evans J., Control of chaos: Methods and applications in engineering, *Annual Reviews in Control*, 29, pp. 33-56, 2005.

[13] Ruiqi W. and Zhujun J., Chaos control of chaotic pendulum system, *Chaos, Solitons and Fractals*, 21(1), pp. 201-207, 2004.

[14] Pecora L. M. and Carroll T. L., Synchronization in chaotic systems, *Physical Review Letters*, 64(8), 821-824, 1990.

[15] Pecora L. M. and Carroll T. L., Synchronizing chaotic circuits, *IEEE Trans. Circuits and Systems*, 38(4), pp. 453-356, 1991.

[16] Wu X. and Lu J., Parameter identification and backstepping control of uncertain Lu system, *Chaos, Solitons and Fractals*, 18(4), pp. 721-729, 2003.

[17] Yu Y. G. and Zhang S. C., Adaptive backstepping synchronization of uncertain chaotic systems, *Chaos, Solitons and Fractals*, 21(3), pp. 643-649, 2004.

[18] Yau H. T., Design of adaptive sliding mode controller for chaos synchronization with uncertainties, *Chaos, Solitons and Fractals*, 22(2), pp. 341-347, 2004.

[19] Wu X., Wang L. and Zhang J., Synchronisation of unified chaotic systems with uncertain parameters in finite time, *International Journal of Modelling, Identification and Control*, Vol 17(4), pp. 295-301, 2012.

[20] Sundarapandian V., Global chaos synchronisation of identical Li-Wu chaotic systems via sliding mode control, *International Journal of Modelling, Identification and Control* Vol 22(2), pp. 170-177, 2014.

[21] Sundarapandian V., Sivaperumal S. and Ahmad T. A., Global chaos synchronisation of identical chaotic systems via novel sliding mode control method and its application to Zhu system, *International Journal of Modelling, Identification and Control* Vol 23(1), pp. 92-100, 2015.

[22] Handa H. and Sharma B. B., Simple synchronisation scheme of chaotic Chua's systems with cubic nonlinearity in complex coupled networks, *International Journal of Applied Nonlinear Science*, Vol 1(4), pp. 300-311, 2014.

[23] Saha P., Ghosh D. and Chowdhury A. R., Modified projective synchronisation of different order chaotic systems with adaptive scaling factor, *International Journal of Applied Nonlinear Science* Vol 1(3), pp. 230-246, 2014.

[24] Chandra Shaker M. and Ghosal A., Nonlinear modeling of flexible link manipulators using nondimensional variables, *Trans. ASME, Journal of Computational and Nonlinear Dynamics*, 1(2), pp. 123-134, 2006.

[25] Nayfeh A. H., *Introduction to Perturbation Techniques*, John Wiley and Sons Inc., 1993.

[26] Endurance Wind Power Ltd., http://www.endurancewindpower.com/e3120.html (last accessed October 6 2016)

[27] MATLAB (2012), *Version 8.0 (R2012b)*, The MathWorks Inc., Natick, Massachusetts.